Geomaterials, 2012, 2, 121-127
http://dx.doi.org/10.4236/gm.2012.24017 Published Online October 2012 (http://www.SciRP.org/journal/gm)

Deformation Stability of Al 7075/20%SiC_p (63 μm) Composites during Hot Compression

M. Rajamuthamilselvan*, S. Ramanathan
Department of Manufacturing Engineering, Annamalai University, Annamalai Nagar, India
Email: *rajanarmi@ yahoo.co.in

Received June 26, 2011; revised August 16, 2011; accepted August 26, 2011

ABSTRACT

In Stir cast Al 7075/20%SiC_p composites were subjected to compression testing at strain rates and temperatures ranging from 0.001 to 1.0 s^{-1} and from 300˚C to 500˚C respectively. And the associated microstructural transformations and instability phenomena were studied by observations of the optical electron microscope. The power dissipation efficiency and instability parameter were calculated following the dynamic material model and plotted with the temperature and logarithm of strain rate to obtain processing maps for strains of 0.5. The processing maps present the instability zones at higher strain rates. The result shows that with increasing strain, the instability zones enlarge. The microstructural examination shows that the interface separates even the particle cracks or aligns along the shear direction of the adiabatic shear band in the instability zones. The domain of higher efficiencies corresponds to dynamic recrystallization during the hot deformation. Using the processing maps, the optimum processing parameters of stain rates and temperatures can be chosen for effective hot deformation of Al 7075/20%SiC_p composites.

Keywords: Composites; Processing Maps; Dynamic Recrystallization; Flow Instability

1. Introduction

Al-based particulate reinforced metal matrix composites (MMC) are recognized as an important class of engineering material due to their lightweight and superior mechanical and thermal properties [1-5]. However, the MMC exhibits poor ductility at room temperature due to the presence of brittle ceramic particles [6,7]. Further studying has found that the MMC can be formed by thermo mechanical processing [8-10]. In order to obtain favorable microstructure and required properties, better control of forming processes is rather essential. The results show that the flow behavior of composite is in direct correlation with the strain rates, temperatures, and deformation degree [11,12]. Therefore, the optimization of the technical parameters will become complicated.

The Processing map based on the theory of dynamic materials model (DMM) is firstly developed by Gegel and Prasad *et al*. and has become a powerful technology for researching the hot-working process of materials [13]. It bridges the continuum mechanics of large plastic deformation and the development of dissipative microstructures in plastic deformation process. It depicts some special microstructural deformation mechanisms, avoid flow instability, optimize deformation process parameters, and obtain desired microstructures and properties. The P-map thus provides rationales for process optimization, product property assurance, microstructure control and defect avoidance [13]. In this paper, the P-map technology is employed to investigate Al 7075/20%SiC_p composites during hot compression at a constant strain rate are conducted. The Processing maps for this alloy are then constructed. Using the Processing maps together with the characterization of microstructure evolution of the alloy in deformation process, the optimal process parameter is identified. The research provides basics and fundamentals for process parameter determination parameter and product quality control in development of Al composites products.

In DMM, a material during hot working is considered as a nonlinear power dissipation system. The power P (per unit volume) absorbed by workpiece in plastic flow process contributes to two types of power consumption. One contributes to the plastic deformation, which in turn leads to the temperature increase in workpiece; the other to microstructure evolution. These two dissipation powers are designatedas G and J, respectively. The G and J are complementary functions and their relationship is represented as [14-16].

$$P = \sigma\dot{\varepsilon} = G + J = \int_0^{\dot{\varepsilon}} \sigma \mathrm{d}\varepsilon + \int_0^{\sigma} \dot{\varepsilon} \mathrm{d}\sigma \qquad (1)$$

Furthermore

*Corresponding author.

$$m=\frac{\partial \log \sigma}{\partial \log \dot{\varepsilon}}\Big/\dot{\varepsilon},T=\left(\frac{\sigma J}{\sigma G}\right)\dot{\varepsilon},T \qquad (2)$$

where m is the strain rate sensitivity factor, which determines the power distribution of P in between the G and J.

In the above equations, G represents the power dissipation of plastic deformation, while J is related to the power needed in microstructure evolution including dynamic recovery, dynamic recrystallization, void formation, and the internal crack generation (wedge cracking, intercrystalline cracking, etc.) in plastic deformation process.

For an ideal linear dissipater, m is equal to 1. J would have the maximum value and $J\max = P/2$. This leads to the definition of a dimensionless parameter and the so-called efficiency of power dissipation, η, given by:

$$\eta = J/J\max = 2m/1+m \qquad (3)$$

The change of η with strain rate ε and deformation temperature constitutes a map called power dissipation map. Its iso-efficiency contours map delineates the variation of the efficiency of power dissipation as a function of $\dot{\varepsilon}$ and deformation temperature. The contours represent the constant efficiency of power dissipation, which is directly related to the relative rate of entropy production in the system by the evolution of microstructure [14]. It also represents the rate of microstructure change in plastic deformation process and the contour is thus termed as the microstructural trajectories. Generally, the high η zone matches the good workability area in the iso-efficiency contours map.

The power dissipation J has a relationship with microstructure evolution and represents the power dissipation in metallurgical evolution process, and the following continuous instable criterion between temperature and strain rate is generated [5,17]:

$$\xi(\dot{\varepsilon})=\frac{\delta \ln\left(m/m+1\right)}{\delta \ln \dot{\varepsilon}}+m \le 0 \qquad (4)$$

The above instability criterion has the physical meaning that if the system is not able to generate entropy at a rate that at least matches the imposed rate, the system will localize the metal flow and cause flow instability. The instability map can be generated by representing the variation of $\xi(\dot{\varepsilon})$ with temperature and $\dot{\varepsilon}$; The P-map can then be constructed by superimposition of the instability map and the power dissipation map. The typical microstructure behaviors in the instable zones predicted by Equation (8) include adiabatic shear band, flow localization, kink band, dynamic strain aging and the mechanical twinning [18-20].

2. Experimental Studies

Stir casting technique was used to fabricate 7075Al alloy reinforced with 15% volume fraction of silicon carbide Composites. The matrix material was 7075 Aluminium Alloy (Composition in wt% Cu 1.66, Mg 2.10, Si 0.14, Mn 0.21, Fe 0.40, Cr 0.18, Zn 5.67, Ti 0.01 and rest Al) and the reinforcement was SiC_p with average size of 63μm. The aluminium alloy was melted by using an Electric Furnace. Preheated SiC_p (250˚C) was added to the melt and mixed by using a rotating impeller in Argon environment and poured in permanent mould. The cast billets were soaked in the temperature of 420˚C for 30 minutes and hot extruded in the ratio of 20:1 [21]. The cylindrical specimens of dimensions, 10 mm in diameter and 10 mm in Height were machined from the extruded rods. The hot compression tests [22] were performed on a 1OT servo controlled universal testing machine for different strains (0.1 - 0.5), strain rates (0.001 s^{-1} - 1.0 s^{-1}) and temperatures (300˚C - 500˚C). Temperature of the specimen was monitored with the aid of a chromel/alumel thermocouple embedded in a 0.5 mm hole drilled half the height of the specimen as stated by Yi Liu *et al*. [23]. The thermocouple was also used for measuring the adiabatic temperature rise in the specimen during deformation. The specimens were effectively lubricated with graphite and deformed to a true strain of 0.5. After compression testing, the specimens were immediately quenched in water and the cross section was examined for microstructure. Specimens were deformed to half of the original height. Deformed specimens were sectioned parallel to the compression axis and the cut surface was prepared for metallographic examination. Specimens were etched with Keller's solution. The microstructure of the specimens was obtained through Versamet 2.0 optical microscope with Clemex vision Image Analyser and mechanism of deformation was studied. Using the flow stress data, power dissipation efficiency and flow instability were evaluated for different strain rates, temperatures at a constant strain of 0.5. The processing maps were developed for 0.5 strains for 7075/Al/15%SiC_p composites.

3. Results and Discussion

3.1. Flow Curves

The flow stress data was generated covering the temperature range of 300˚C - 500˚C and strain rate range 0.001 - 1.0 s^{-1} from compression testing of solid cylinders of size 10 mm in diameter and 10 mm in height using servo hydraulic testing machine capable of imposing constant true strain rates on the specimen. Adiabatic temperature rise during high strain rate testing was measured and the flow stress was corrected for the temperature rise. The specimens were compressed to 50% of their initial height and the load-stroke curves obtained in the hot compression were converted in to true stress-true

plastic strain curves by subtracting the elastic portion of the strain and using the standard equations for the true stress and true strain calculations. The values of the efficiency parameter (η) and the strain rate sensitivity parameter (m) to use the instability condition are determined from the flow stress test data of the material.

Typical true stress-true strain curves obtained for different strain rates and constant temperature are given in **Figure 1**. At 0.1 s^{-1} strain rate, the flow stress reaches a peak at a critical strain and then sharply decreases to a steady value at the temperature of 450˚C. The characteristics of this flow stress curves demonstrate the happening of DRX. Generally, DRX is a beneficial process in hot deformation since it not only gives stable flow and good workability to the material by simultaneously softening it but also reconstitutes the microstructure [24].

Therefore, it is observed that the flow stress is in direct correlation with the strain rates. The variation of stress is related to a variation in dislocation density as well as the formation and development of sub grain boundaries, which result from working hardening and softening mechanism. At lower strain rates, the deformation is isothermal but at high strain rates it is adiabatic [25]. This phenomenon at higher strain rate deformation is the consequence of the inadequate heat dissipation. Further, this leads to an increase in work hardening rate at higher strain rate deformation. However, at lower strain rate, the strain hardening is almost compensated by softening due to higher temperature. Hence, near steady state flow curve is observed.

Typical true stress vs true strain curves at different temperatures with strain rate of 0.1 s^{-1} are shown in **Figure 2**. It can be seen that the flow stress decreases with increasing temperature and decreasing strain rate, thereby, exhibiting typical behaviour of metal deformed under hot working conditions. True stress vs true strain curve at 450˚C exhibits work hardening (**Figure 2**) whereas at higher temperature the flow softening is observed after a critical strain. The curves are characterized by an initial sharp increase of flow stress with strain up to a certain value that is followed by slope of flow decreasing and very limited flow softening [26]. From the mentioned flow stress-strain character, it can be concluded that the work-hardening effect is pronounced at low temperatures. Generally, during the deformation the matrix around the SiC particles presents much higher dislocation density than that of normal alloy. The high dislocation density regions restrict the plastic flow and contribute to a competing behavior between dynamic softening and the work hardening.

3.2. Processing Map

Processing maps were developed and shown in **Figure 3** by superimposing contour plots of instability parameter

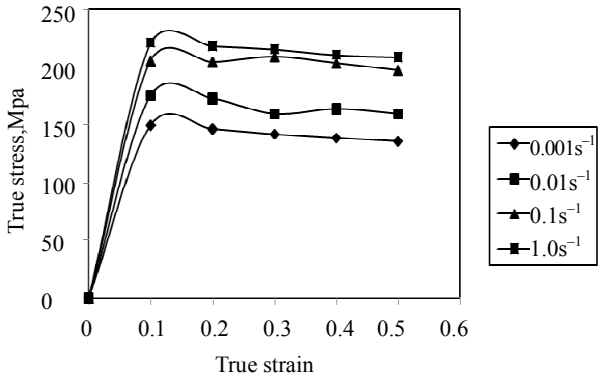

Figure 1. The flow curves of 7075 Al/20%SiC_p (63 µm) for different strain rates at constant temperature of 450˚C.

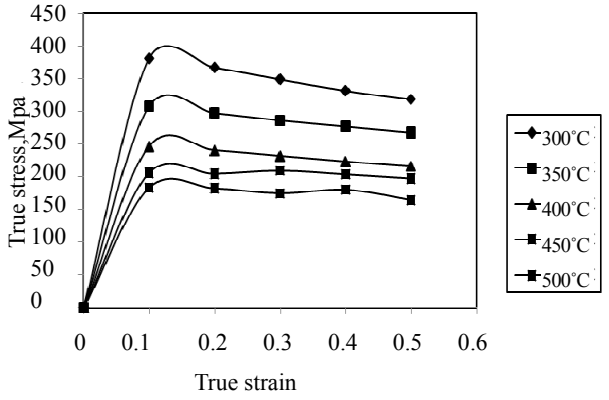

Figure 2. The flow curves of 7075 Al/20%SiC_p (63 µm) for different temperatures at constant strain rate of 0.1 s^{-1}.

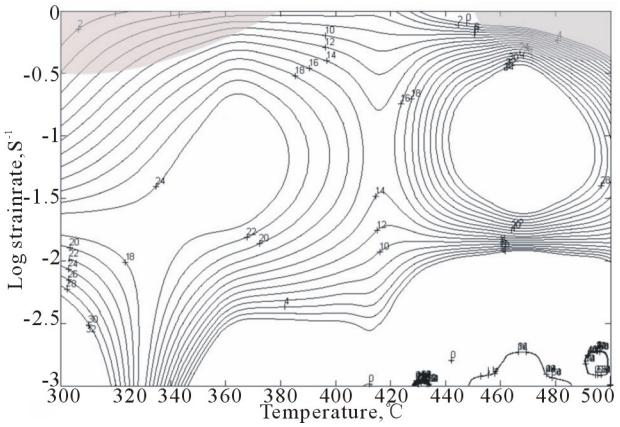

Figure 3. Processing map at 0.5 strains.

on those of power dissipation efficiencies. The approach of processing map has been introduced to study the deformation mechanisms and to optimize hot forming process for this material. These maps show the stable and unstable deformation in the processing space on the axes of temperatures and strain rates. It is helpful to understand the interaction effects between strain rates and temperatures. Consequently, the components with con-

trolled microstructure and properties can be manufactured without macro or micro defects. In the process maps, the contour numbers represent efficiency of power dissipation and shaded region corresponds to flow instability [10].

The contour numbers represent the valves of the instability parameter $\xi(\dot{\varepsilon})$ in the instability maps. It can be noted that the values of parameter $\xi(\dot{\varepsilon})$ are negative at the lower deformation temperature and higher strain rate; with increasing strain, the region of negative contour becomes larger. The region in which the value of parameter $\xi(\dot{\varepsilon})$ becomes negative suggests the possibility of unstable flow. The greater the negative magnitude of $\xi(\dot{\varepsilon})$, the higher the possibility of unstable flow.

Figure 3 illustrates the contour maps of strain rate sensitivity and efficiency of power dissipation calculated at strain 0.5. If the values of m and η are negative, the material presents some types of unstable flows. Furthermore, it is generally considered that higher values of m and η reduce the tendency for flow localization and result in the maximum ductility. The contour maps for strain rate sensitivity parameter and efficiency of power dissipation, corresponding to strains of 0.5 exhibit interesting domain. The domain of η maps occurs in the temperature range of 445˚C to 485˚C and strain rate range of 0.018 s^{-1} to 0.16 s^{-1}. The maximum values of η for strains of 0.5 in this domain have increased up to 34% at the deformation temperature of 450˚C with strain rate of 0.1 s^{-1}.

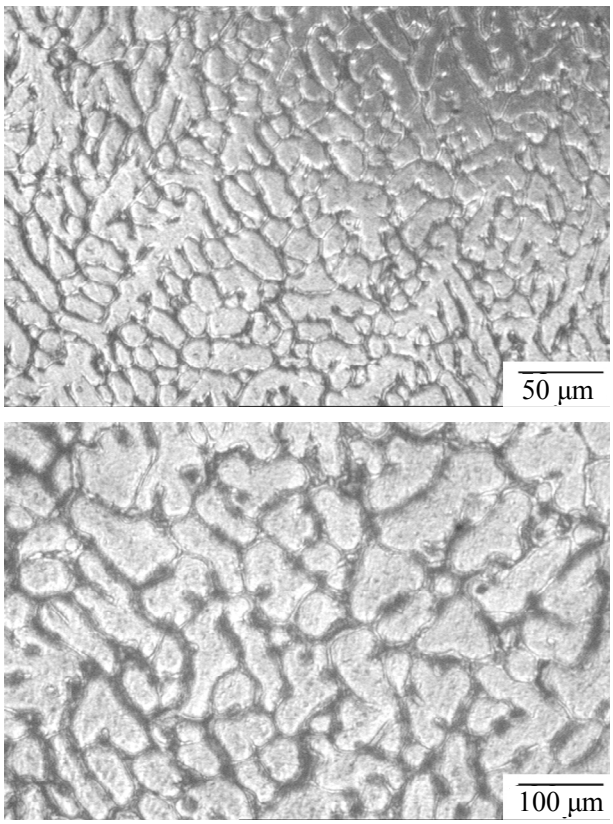

Figure 4. Dynamic recrystallization at 450˚C at a strain rate of 0.1 s^{-1}.

3.3. Microstructure Examinations

3.3.1. Instability Zones

Dynamic recrystallization (DRX) observed at 450˚C with strain rate of 0.1 s^{-1} are presented in **Figure 4**. The flow curves in this domain represent oscillations in the flow curves before reaching steady state. The microstructure has higher density dislocation domains and dislocation cell structures. And the more complex dislocation structures were formed around SiC particles. The high dislocation density regions restrict the plastic flow and contribute to the strengthening and strain hardening. The flow curves exhibit work hardening at 450˚C with strain rate of 0.1 s^{-1}. The flow deformation behavior mainly presents working hardening under this condition. As the temperature increases, the strengthening effect of sic is considerably diminished, so that the material shows a similar softening behavior of the pure metals. In **Figure 4**, it can be seen that uniform and fine grains were formed, which can be attributed to the occurrence of dynamic recrystallization (DRX). DRX is a beneficial process in hot deformation as it gives good intrinsic workability by simultaneous softening and reconstituting the microstructure. Therefore, DRX is a chosen domain for hot workability optimization and good microstructure control in the safe zone. So, the optimum processing parameters attained by the maps are the temperature and strain rate ranges of 445˚C - 485˚C and 0.018 s^{-1} - 0.16 s^{-1}, respectively. Traditionally, DRX is associated with hot working of low stacking fault energy (SFE) metals which exhibit flow softening after reaching a critical strain. Aluminium is a high stacking fault energy material and is characterized by easy dislocation climb and cross slip during deformation. However, the added SiC particles affect the density and distribution of dislocations in the matrix, and may influence the driving force for recrystallization. In addition, the accumulation of dislocations in the vicinity of SiC particles may lead to the fact that those regions become sites for recrystallization nucleation.

Dynamic recrystallization thus becomes easier to occur. Hence, the domain can be interpreted to represent the region of possible dynamic recrystallization [5,27,28]. Elongation obtained on the specimens deformed at temperature of 450˚C and strain rate of 0.1 s^{-1} are shown in **Figure 5**.

3.3.2. Instability Zones

Figure 6 shows the particles alignment along the shear direction at 300˚C with the strain rate of 1.0 s^{-1} for strain of 0.5. At higher strain rates, since the time is short,

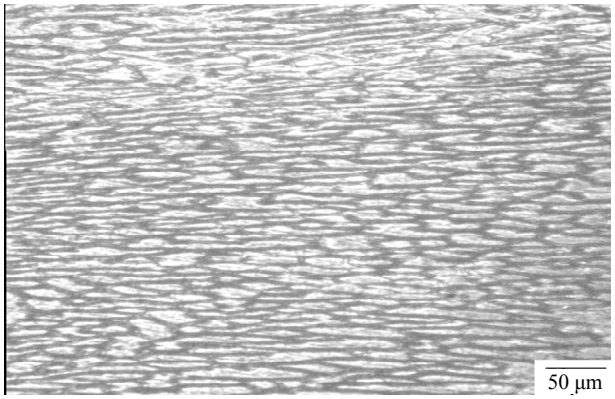

Figure 5. Grain elongation at 450˚C and at a strain rate of 0.01 s^{-1}.

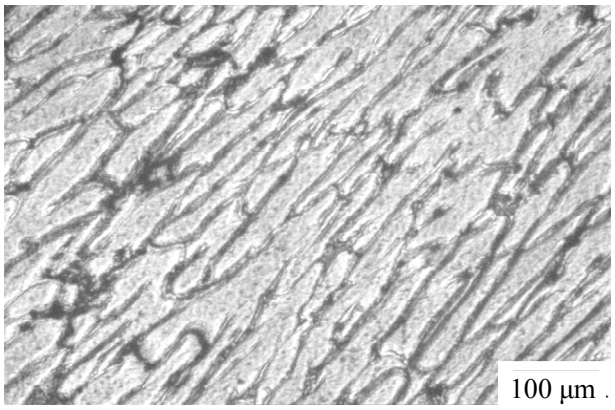

Figure 6. Shear band formation at 300˚C and at a strain rate of 1.0 s^{-1}.

conducted away to the colder parts of the body, a drop in the flow stress occurs locally and therefore slip becomes localized [30]. This is called adiabatic shear bands which exhibit cracking, recrystallization along macroscopic shear planes and this generally occurs sharply at 45˚ with respect to the principal stress axis [5]. The SiC present in the aluminium matrix is disturbed due to the flow of matrix in the shear direction. So, the particles alignment along the shear directions is observed. The flow localization is due to the interface cracking or the SiC particle itself breaking and adiabatic shear bands present in the metal matrix, which are the manifestations of flow instability predicted by the instability maps. Therefore, those flow instability regions must be avoided.

The interface cracking observed at 500˚C with the strain rate of 1.0 s^{-1} is shown in **Figure 7**. The presence of SiC particles in aluminum matrix during deformation causes the interface to crack since the matrix undergoes plastic flow while the particles do not deform [29]. As a result, the accumulated stress will emerge at the interface between the matrix and the particles. When the accumulated stress becomes large, the interface may separate at relatively lower temperature and higher strain rates. The

Figure 7. SEM image of interface cracking at 500˚C and a strain rate of 1.0 s^{-1}.

particle breakage is due to accumulated stress at the interface exceeding the yield stress of the particle; hence, this results in particle breakage [28].

It is concluded that with increasing strain, the flow instability manifestation of composites becomes more significant at higher stain rate, owing to increased defects such as particle fracture, debonding and adiabatic shear band. The stable deformation mechanisms include elongation and DRX. The occurrence of DRX at higher temperatures and moderate strain rate deformation results in flow stress decreasing in those deformation ranges.

4. Conclusions

1) Hot compression tests were performed on Al/20% SiC composites produced through Stir casting technique. The flow stress was evaluated for a temperature range of 300˚C - 500˚C and a strain rate range of 0.001 - 1.0 s^{-1}. The power dissipation efficiency and instability parameters were evaluated and processing maps were constructed for 0.5 strains. The optimum domains and instability zone were obtained for the material.

2) The optimum processing parameters attained by the maps are the temperature and strain rate ranges of 445˚C - 485˚C and 0.018 s^{-1} - 0.16 s^{-1}, respectively. Dynamic recrystallization (DRX) observed at 450˚C with strain rate of 0.1 s^{-1}.

3) The processing maps present the instability zones at higher strain rate; and with increasing strain, the instability zones enlarge. The microstructural examination shows that composites exhibit flow localization as bands of flow localizations, the interface cracking and particle breakage.

After the text edit has been completed, the paper is ready for the template. Duplicate the template file by using the Save As command, and use the naming convention prescribed by your journal for the name of your paper. In this newly created file, highlight all of the con-

tents and import your prepared text file. You are now ready to style your paper.

5. Acknowledgements

The authors are grateful to The Department of Manufacturing Engineering, Annamalai University, Tamilnadu, India for the support rendered for the fabrication and testing of Composites

REFERENCES

[1] H. R. Hafizpour, M. Sanjari and A. Simchi, "Analysis of the Effect of Reinforcement Particles on the Compressibility of Al-SiC Composite Powders Using a Neural Network Model," *Materials and Design*, Vol. 30, 2009, pp. 1518-1523.

[2] N. Chawla, X. Deng and D. R. M. Schnell, "Thermal Expansion Anisotropy in Extruded SiC Particle Reinforced 2080 Aluminum Alloy Matrix Composites," *Materials Science and Engineering A*, Vol. 426, 2006, pp. 314-322.

[3] D. B. Miracle, "Metal Matrix Composites—From Science to Technological Significance," *Composite Science and Technology*, Vol. 65, 2005, pp. 2526-2540.

[4] S. Basavarajappa and G. Chandramohan, "Application of Taguchi Techniques to Study Dry Sliding Wear Behaviour of Metal Matrix Composites," *Materials and Design*, Vol. 28, 2007, pp. 1393-1398.

[5] S. Ramanathan, R. Karthikeyan and G. Ganasen, "Development of Processing Maps for 2124Al/SiC_p Composites," *Materials Science and Engineering A*, Vol. 441, 2006, pp. 321-325.

[6] D. P. Mondal, S. Das and K. S. Suresh, "Compressive Deformation Behaviour of Coarse SiC Particle Reinforced Composite: Effect of Age-Hardening and SiC Content," *Materials Science and Engineering A*, Vol. 460, 2007, pp. 550-560.

[7] Z. Xue, Y. Huang and M. Li, "Particle Size Effect in Metallic Materials: A Study by the Theory of Mechanism-Based Strain Gradient Plasticity," *Acta Materialia*, Vol. 50, 2002, pp. 149-160.

[8] G. Ganesan, K. Raghukandan and R. Karthikeyan, "Development of Processing Map for 6061 Al/15%SiC_p through Neural Networks," *Journal of Materials Processing Technology*, Vol. 166, 2005, pp. 423-429.

[9] S. V. S. N. Murty, B. N. Rao and B. P. Kashyap, "On the Hot Working Characteristics of 6061 Al-SiC and 6061-Al_2O_3 Particulate Reinforced Metal Matrix Composites," *Composites Science and Technology*, Vol. 63, 2003, pp. 119-135.

[10] E. Cerri, S. Spigarelli and E. Evangelista, "Hot Deformation and Processing Maps of Particulate-Reinforced 6061 + 20% Al_2O_3 Composite," *Materials Science and Engineering A*, Vol. 324, 2002, pp. 157-161.

[11] K. S. See and T. A. Dean, "The Effects of the Disposition of SiC Particles on the Forgeability and Mechanical Properties of Co-Sprayed Aluminium-Based MMCs," *Journal of Materials Processing Technology*, Vol. 69, 1997, pp. 58-67.

[12] V. C. Srivastava, V. Jindal and V. Uhlenwinkel, "Hot-Deformation Behaviour of Spray-Formed 2014 Al + SiC_p Metal Matrix Composites," *Materials Science and Engineering A*, Vol. 477, 2008, pp. 86-95.

[13] P. S. Robi and U. S. Dixit, "Application of Neural Networks in Generating Processing Map for Hot Working," *Journal of Materials Processing Technology*, Vol. 142, 2003, pp. 289-294.

[14] Y. V. R. K. Prasad, "Processing Maps: A Status Report," *Material Engineering and Performance*, Vol. 12, No. 6, 2003, pp. 638-645.

[15] M. Q. Li, H. S. Pan, Y. Y. Lin and J. Luo, "High Temperature Deformation Behavior of near Alpha Ti-5.6Al-4.8Sn-2.0Zr Alloy," *Journal of Materials Processing Technology*, Vol. 183, 2007, pp. 71-76.

[16] D. Y. Cai, L. Y. Xiong, W. C. Liu, G. D. Sun and M. Yao, "Development of Processing Maps for a Ni-Based Superalloy," *Material Characterization*, Vol. 58, 2007, pp. 941-946.

[17] Y. V. R. K. Prasad and S. Sasidhara, "Hot Working Guide," ASM International, Materials Park, 1997.

[18] C. Y. Wang, X. J. Wang, H. Chang, K. Wu and M. Y. Zheng, "Processing Maps for Hot Working of ZK60 Magnesium Alloy," *Materials Science and Engineering A*, Vol. 464, 2007, pp. 52-58.

[19] W. Wang, Y. Zhang, X. Zeng and W. Ding, "Characterization of Dynamic Recrystallisation in As-Homogenized Mg-Zn-Y-Zr Alloy Using Processing Map," *Journal of Material Science*, Vol. 41, 2006, pp. 3603-3608.

[20] P. K. Sagar, "Effect of Alloying Elements and Microstructure on the Processing Parameters of $\alpha 2$ Aluminide Alloys," *Materials Science and Engineering A*, Vol. 434, 2006, pp. 259-268.

[21] W. H. Yuan, J. Zhang, C. C. Zhang and Z. H. Chen, "Processing of Ultrahigh Strength SiC_p/Al-Zn-Mg-Cu Composites," *Journal of Materials Processing Technology*, Vol. 209, 2009, pp. 3251-3255.

[22] Y. C. Lin, M.-S. Chen and J. Zhong, "Prediction of 42 CrMo Steel Flow Stress at High Temperature and Strain Rate," *Mechanics Research Communications*, Vol. 35, No. 3, 2008, pp. 142-150.

[23] Y. Liu, R. Hu, J. S. Li, H. C. Kou, H. W. Li, H. Chang and H. Z. Fu, "Characterization of Hot Deformation Behavior of Haynes230 by Using Processing Maps," *Journal of Materials Processing Technology*, Vol. 209, 2009, pp. 4020-4026.

[24] Z. Yang, Y. C. Guo and J. P. Li, "Plastic Deformation and Dynamic Recrystallization Behaviors of Mg-5Gd-4Y-0.5Zn-0.5Zr Alloy," *Materials Science and Engineering A*, Vol. 485, 2008, pp. 487-491.

[25] S. Ramanathan, R. Karthikeyan and M. Gupta, "Development of Processing Maps for Al/SiC_p Composite Using Fuzzy Logic," *Journal of Materials Processing Technology*, Vol. 183, 2007, pp. 104-110.

[26] X. M. He, Z. Q. Yu and X. M. Lai, "A Method to Predict Flow Stress Considering Dynamic Recrystallization during Hot Deformation," *Computational Material Science*,

Vol. 44, 2008, pp. 760-764.

[27] P. Cavaliere and E. Evangelista, "Isothermal Forging of Metal Matrix Composites: Recrystallization Behaviour by Means of Deformation Efficiency," *Composites Science and Technology*, Vol. 63, 2003, pp. 119-135.

[28] G. Ganesan, K. Raghukandan, R. Karthikeyan and B. C. Pai, "Development of Processing Maps for 6061 Al/15% SiC_p Composite Material," *Materials Science and Engineering A*, Vol. 369, 2004, pp. 230-235.

[29] Y. W. Yan, L. Geng and A. B. Li, "Experimental and Numerical Studies of the Effect of Particle Size on the Deformation of the Metal Matrix Composites," *Materials Science and Engineering A*, Vol. 448, 2007, pp. 315-325.

[30] P. Cavaliere, E. Cerri and P. Leo, "Hot Deformation and Processing Maps of a Particulate Reinforced 2618Al_2O_3/20p Metal Matrix Composite," *Composites Science and Technology*, Vol. 64, 2004, pp. 1287-1291.

